Electron radiation damage and Li-colloid creation in Li_2O

P. Vajda and F. Beuneu
Laboratoire des Solides Irradiés, CNRS-CEA, Ecole Polytechnique F-91128 Palaiseau, France
(Received 12 October 1995)

Polycrystalline samples of Li_2O were irradiated with 1-MeV electrons at different temperatures, T_{irr}, in the range 21 to 275 K, and their electron paramagnetic resonance spectra measured. The created defects manifest a strong T_{irr} dependence. (i) At low temperatures, $T_{irr} \lesssim 200$ K, mainly F^+ centers (O vacancies with a trapped electron) are formed; thermal annealing leads to their recovery near $T_{ann} = 400$ °C, which is accompanied by the emergence of a new signal near $g = 2.003$, possibly due to their agglomeration into small F^+ clusters. The latter disappear at 600–700 °C. (ii) At $T_{irr} = 200$ K, the F^+ spectra are superimposed by the $g = 2.003$ line and by a new narrow signal at $g = 2.0023$, probably already caused by small metallic colloids. (iii) At $T_{irr} = 275$ K, finally, only a narrow T-independent line ($\Delta H \sim 10^{-2}$ mT) is observed at $g = 2.00235(2)$, characteristic for metallic Li colloids. The microwave dielectric constant, ε, measured on the same specimens increased notably after the room-temperature irradiation emphasizing the presence of metallic particles, while remaining unchanged for lower T_{irr}. Both the colloid line and the radiation-induced $\Delta\varepsilon$ vanish simultaneously above $T_{ann} \approx 250$ °C.

I. INTRODUCTION

Lithium is one of the few metals[1] whose conduction electrons yield a signal in electron-spin-resonance (CESR) and has, therefore, drawn particular experimental and theoretical attention already in the early CESR days.[2] For the same reason, it was also a much studied candidate for metallic colloid formation in ionic crystals (for a review, see, e.g., Ref. 3). Thus, after the pioneering work on neutron-irradiated LiF (of NaCl structure), where Li colloids had been detected by x rays,[4] NMR,[5] and EPR,[6] and later by differential thermal analysis,[7] they were also observed more recently in optical absorption work on Ar- and Ne-ion implanted LiF samples[8] and on the surface of low-energy electron bombarded LiF crystals.[9] The other system where Li colloids were reported unambiguously is its crystallographic analogue LiH. There, metallic lithium was formed by additive coloring through exposure to uv light and detected by electron paramagnetic resonance (EPR) and optical absorption by Doyle, Ingram, and Smith,[10] while Pretzel *et al.*[11] observed them in LiT-containing LiH exposed to β radiation from the tritium decay; Berthault, Bedere, and Matricon[12] reported a CESR line in γ-irradiated LiH.

The radiation stability of Li_2O (of antifluorite structure) has been studied intensively since its establishment as a prospective first-wall cladding material in fusion reactors, due to the tritium breeding properties of the lithium nucleus. Most of the radiation damage work was done by Noda and coworkers in the Japanese Atomic Energy Research Institution, where detailed studies were performed on Li_2O bombarded with fast and thermal neutrons,[13–17] by high-energy oxygen ions,[18–20] and lithium ions.[21] The observations were interpreted by the creation and evolution of F^+ centers (oxygen vacancies with a trapped electron). Asaoka *et al.*[22] investigated the luminescence spectra in Li_2O irradiated with 2-MeV He^+ ions, and Baker *et al.*[23] described an EPR signal due to interstitial hydrogen, H^0, after x-ray irradiation. No Li colloids were reported until now in irradiated Li_2O, except by Noda and co-workers[13,16,17,19] where an occasional extra line near $g = 2.003$ in their EPR spectra was claimed to be caused by metallic Li clusters, mainly because of its isotropic character. (We shall show later in this work that this line is not due to Li colloids but most probably to small nonmetallic aggregates of F^+ centers.)

In the present work, where we have succeeded to create metallic lithium colloids by energetic electron irradiation of Li_2O and to observe them by means of CESR and microwave conductivity measurements, we shall determine the conditions for their formation from the primary defects, which appear to be the F^+ centers. At the same time, we shall describe the formation and evolution of the latter under electron irradiation and subsequent annealing and compare our results with data obtained after heavy-particle irradiation. The following results concern primarily polycrystalline material; the analysis of single-crystal work is in progress and shall be published in the future. Preliminary data were communicated at the REI-8 conference on radiation effects in insulators in Catania.[24]

II. EXPERIMENTAL TECHNIQUES

The specimens were prepared from nominally 99.5% pure polycrystalline Li_2O grains, purchased from Cerac Inc. (Milwaukee, WI), which contained according to the supplier 0.08 at. % Al, 0.02 Si, and less than 0.01 at. % Ba, Ca, Cr, Cu, Fe, Mg, Mn, Sr, and Ti, each. 0.5 mm thick platelets of about 5×2 mm^2 size were cut from the grains and annealed in a vacuum of $< 10^{-6}$ Torr for 5 hours at 900 °C to eliminate residual LiOH and Li_2CO_3. For irradiation purposes, the samples were wrapped in a 10 μm thick copper foil fixed to a holder and transferred to a liquid-hydrogen cryostat attached to our Van de Graaff electron accelerator. The employed beam energy was 1 MeV; this ensures a uniform damage distribution in our samples, as only ~150 keV are lost by 1 MeV electrons in 0.5 mm Li_2O.[25] The irradiation temperature was controlled by regulating the beam current and/or a

heater positioned above the hydrogen bath and measured with a copper-constantan thermocouple soldered to the copper foil. In this experiment, we had applied the following irradiation temperatures: $T_{\rm irr}=21(1)$ K, 90(5) K, 150(3) K, 200(2) K, and 275(3) K. After irradiation, the samples were kept in liquid nitrogen if necessary, but were extracted at room temperature for the measurements.

For defect detection, X-band EPR experiments were performed on a Bruker ER200D spectrometer between 4 and 300 K. Furthermore, microwave conductivity measurements were done on the same specimens, using a TE_{10n} cavity with eight useful resonant modes in the range 7–15 GHz; the measurement, with an HP8510C network analyzer, of the shift in frequency, Δf, and of the Q factor, $\Delta(Q^{-1})$, permitted to determine the real and the imaginary parts of the dielectric constant, $\varepsilon=\varepsilon'-i\varepsilon''$.

A thermal annealing treatment was applied to the specimens by heating them in a dynamic vacuum in steps of 50°, for one hour each, up to the disappearance of the introduced damage.

In addition, the sample quality and its evolution with the various treatments, was checked by x-ray diffraction on identical Li_2O specimens irradiated simultaneously in the same copper bag with their twin.

III. EXPERIMENTAL RESULTS

In the present section, we shall describe the results obtained after electron irradiation at various temperatures, $T_{\rm irr}$, between liquid-hydrogen and room temperature and the subsequent recovery behavior of the samples, organized in subsections according to the different $T_{\rm irr}$. Note that the intensities of all the lines (as used in Figs. 2, 3, 5, 7, and 9) are taken in the same, though arbitrary, units and are, therefore, comparable with each other.

A. $T_{\rm irr}=21$ K

A typical EPR spectrum obtained after a low-temperature irradiation with a beam current of 40 μA/cm^2 and a fluence of 0.8×10^{20} e^-/cm^2, is shown in the upper part of Fig. 1. It corresponds to that of the F^+ center observed by Noda *et al.* after heavy-particle irradiation[15,16,19] and exhibits the 25 lines of the hyperfine structure due to the cubic environment of an oxygen vacancy surrounded by eight Li^7 ($I=\frac{3}{2}$) nuclei as first neighbors. Upon heating above room temperature, the F^+ signal decreases gradually and a central line emerges simultaneously at $g=2.0030(2)$, with a width of $\Delta H\sim0.5$ mT. The latter has reached its maximum after annealing at $T_{\rm ann}=400$ °C, when the F^+ spectrum has nearly vanished (lower part of Fig. 1). The differing origin of the central line is clearly seen in the different saturation behavior of its intensity, I_c, when compared to that of its first neighbor to the left, I_{c-1}, demonstrated in Fig. 2, for several measuring temperatures, T_m, as parameter; the F^+ signal, represented by I_{c-1}, saturates at much lower microwave power than the central line, I_c. All signals exhibited Curie-like behavior with temperature.

The global annealing behavior of the two lines, I_c and I_{c-1}, is represented in Fig. 3. For easier visualization, we have also drawn the difference, $\Delta I=I_c-I_{c-1}$ for each $T_{\rm ann}$, indicating the maximum of the central line at 400 °C

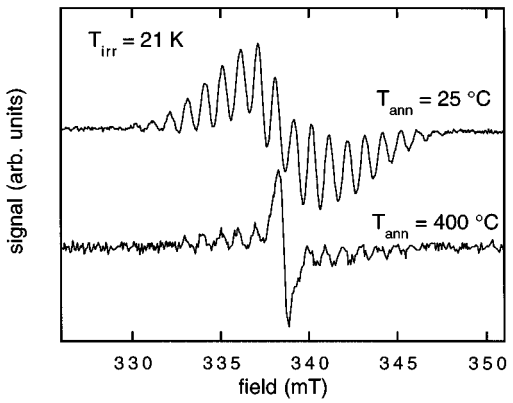

FIG. 1. Room-temperature EPR spectra of Li_2O irradiated at 21 K by 1-MeV electrons to a dose of 0.8×10^{20} e^-/cm^2. Upper spectrum: after irradiation; microwave attenuation $P=34$ dB (corresponding to a power of 100 μW), modulation $M=0.2$ mT. Lower spectrum: after an anneal at $T_{\rm ann}=400$ °C; $P=28$ dB (400 μW), $M=0.2$ mT.

and its progressive disappearance until $T_{\rm ann}\sim600$ °C. Note also the simultaneous decrease of the I_c-linewidth from $\Delta H\sim0.5$ to 0.1 mT. Finally, we wish to mention that the originally white specimen, which had become dirty yellowish (khaki-like) after irradiation, has turned gray-black during the anneal (darkest after $T_{\rm ann}=400$ °C), before bleaching again for higher temperatures. The dielectric constant remained unchanged after irradiation, $\varepsilon_0'=6.0(3)$ and $\varepsilon_0''=0.01(1)$.

B. $T_{\rm irr}=90$ K and 150 K

The results of the two irradiations (with a beam current of 10 μA/cm^2 and a fluence of 0.3×10^{20} e^-/cm^2 at $T_{\rm irr}=90$ K, and 20 μA/cm^2 and 0.65×10^{20} e^-/cm^2 at $T_{\rm irr}=150$ K) were qualitatively similar, and we shall present them together, stressing occasional differences when appropriate. Figure 4 exhibits room-temperature EPR spectra immediately after irradiation (the upper and central parts), for both $T_{\rm irr}$, and,

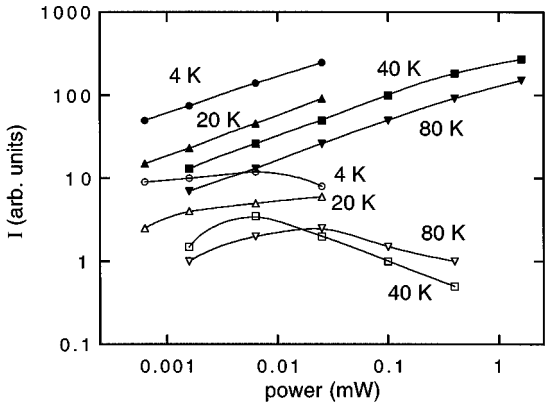

FIG. 2. Intensity as a function of microwave power for the central line, I_c (full signs), and for its first neighbor to the left, I_{c-1} (empty signs), after irradiation at 21 K and annealing at 400 °C, at various measuring temperatures, T_m, indicating different saturation behavior of the two lines.

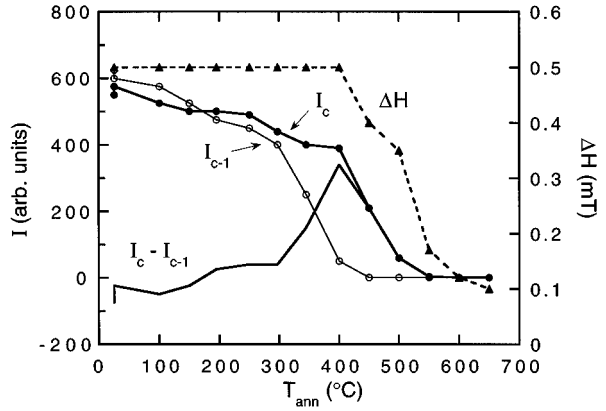

FIG. 3. Annealing of the spectra of Fig. 1, giving the intensity recovery of I_c, of I_{c-1}, and of the difference, $I_c - I_{c-1}$. The evolution of the linewidth, ΔH, of the central line is also shown.

after an anneal at 450 °C (lower part), for the representative $T_{irr}=90$ K case. One notes that, in both irradiations, F^+ centers are created, which are transformed into the defect characterized by the central line at $g=2.0030$ upon annealing. A significant difference between the two irradiations is the somewhat more complex spectrum after $T_{irr}=150$ K (central part of Fig. 4) as if superimposed by another line in the center—in that case the $g=2.003$ line showing up already at 25 °C.

Figure 5 presents the annealing behavior of the two line intensities, I_c and I_{c-1}, together with their difference $\Delta I = I_c - I_{c-1}$, as a function of temperature, for $T_{irr}=90$K. As the maximum of the central line emerges, this time, after $T_{ann}=450$ °C, it turns out to be better separated from the F^+ signal than after the irradiation at $T_{irr}=21$ K (Fig. 3). Moreover, its linewidth ΔH tends to increase again with T_{ann} above 500 °C, from $\Delta H \sim 0.15$ to 0.3 mT. The F^+ signal disappears in both cases at 400 °C, the $g=2.003$ line vanishes progressively until 750 °C. Like in the first case, the emergence of the central line after an anneal at 350–400 °C is accompanied by a striking color change of the sample, from khaki to gray-black.

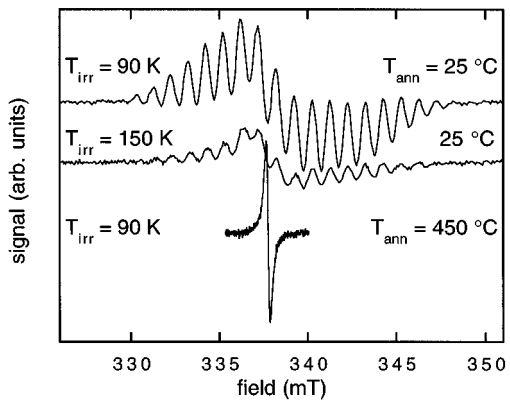

FIG. 4. Room-temperature EPR spectra of Li_2O irradiated at 90 K and at 150 K, with 0.3 and 0.65×10^{20} e^-/cm^2, respectively; $P=22$ dB (1.6 mW). (a) after irradiation at 90 K, $M=0.2$ mT; (b) after irradiation at 150 K, $M=0.2$ mT; (c) $T_{irr}=90$ K, after annealing at 450 °C, $M=0.1$ mT.

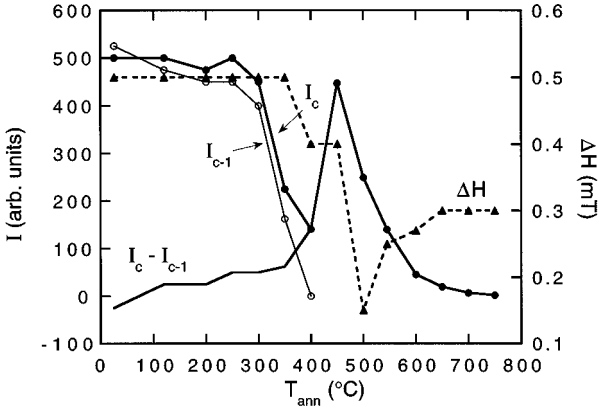

FIG. 5. Same as in Fig. 3, for $T_{irr}=90$ K.

C. $T_{irr}=200$K

Increasing the irradiation temperature to 200 K (with a beam current of 25 μA/cm^2 and a fluence of 0.6×10^{20} e^-/cm^2) leads to an increase of the central complex structure with respect to the still present but strongly diminished "normal" F^+ signal (Fig. 6, upper spectrum). But, most interesting, one notes an additional narrow line ($\Delta H \sim 0.05$ mT) at $g=2.00232$ to 2.00235, close to the free-electron value. Unlike all the other signals present, this line exhibits no Curie-like temperature dependence and could be a first manifestation of small metallic colloids.

The high-frequency dielectric constant, which had remained the same after the three lower-temperature irradiations, seem, this time, to have increased slightly to $\varepsilon'=7.0(3)$ and $\varepsilon''=0.02(1)$. This is close to the limit of our measuring sensitivity but appears credible, in view of the equally modified sample color: it has turned dark-gray right after irradiation, instead of khaki as before.

The annealing behavior is summarized in Fig. 7, and a selected spectrum after $T_{ann}=350$ °C is shown in the lower part of Fig. 6. The F^+ signal vanishes at 400 °C, the central line grows strongly until $T_{ann}=350$ °C and decreases thereafter together with its linewidth up to 600 °C. The intensity

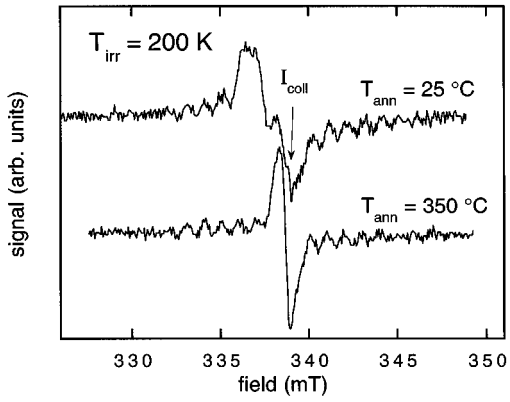

FIG. 6. Room-temperature EPR spectra of Li_2O irradiated at 200 K with 0.6×10^{20} e^-/cm^2. Upper spectrum: after irradiation; $P=20$ dB (2.5 mW), $M=0.1$ mT. Lower spectrum: after an anneal at $T_{ann}=350$ °C; $P=26$ dB (625 μW), $M=0.2$ mT. Note the presence of a narrow colloid line at $g=2.0023$, after irradiation.

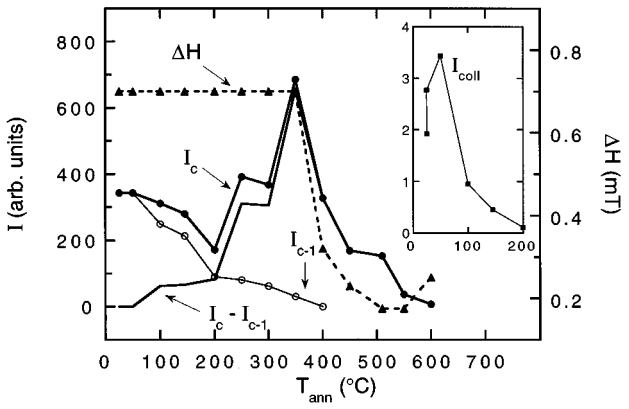

FIG. 7. Same as in Fig. 3, for $T_{irr}=200$ K. The intensity evolution of the colloidal line at $g=2.0023$ with T_{ann} is shown in the inset.

of the colloid line, I_{coll}, grows until a $T_{ann}=50$ °C before disappearing at 200 °C (inset of Fig. 7); its linewidth has a slight tendency, if any, to increase with T_{ann}, in contrast to that of the central, I_c, line.

D. $T_{irr}=275$ K

An irradiation close to room temperature (Fig. 8 beam current 40 μA/cm^2 and a fluence of 1.1×10^{20} e^-/cm^2) has now led to a qualitatively new situation. Instead of the hyperfine structure of the F^+ center one observes only a very narrow ($\Delta H\leqslant 0.01$ mT) line, which has all characteristics of a signal due to metallic lithium: it is positioned at $g=2.00234$ to 2.00238; its intensity follows a Pauli law—the T independence is shown in the inset of Fig. 8, with an equally T-independent linewidth; it is isotropic, according to preliminary results obtained with a single crystal. The line is somewhat broad at the wings and a good fit requires at least two Lorentzians, indicating the probable presence of colloids

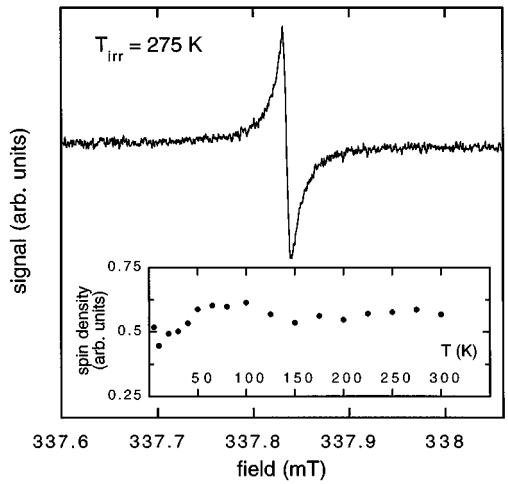

FIG. 8. Upper part: room-temperature EPR spectrum of Li_2O irradiated at 275 K with 1.1×10^{20} e^-/cm^2; $P=32$ dB (156 μW), $M=0.005$ mT. Inset: T dependence of the signal, showing Pauli behavior of its intensity.

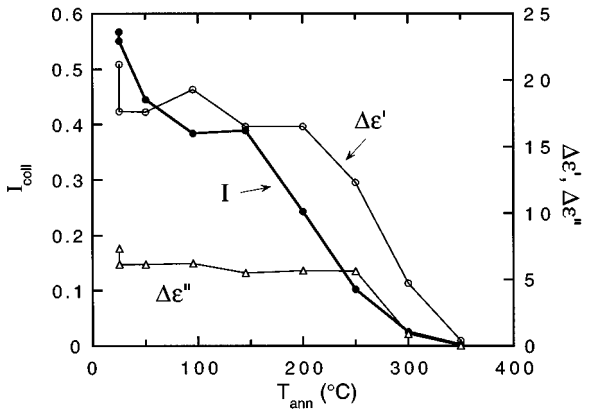

FIG. 9. Annealing of the intensity of the colloid line of Fig. 8 (its linewidth remains constant), together with the evolution of the radiation-induced changes in the real and in the imaginary parts of the dielectric constant, $\Delta\varepsilon'$ and $\Delta\varepsilon''$ [$\varepsilon'_0=6.0(3)$, $\varepsilon''_0=0.01(1)$, before irradiation].

of various sizes. The line shape is definitely not dysonian, which is consistent with a colloid size below the micron range.

Most impressive, however, is the striking simultaneous increase of the dielectric constant. The sample, which has turned black after the irradiation, exhibits now an $\varepsilon'_{irr}=27$ and $\varepsilon''_{irr}=7$, suggesting in a convincing manner the presence of metallic particles. In particular, the notable ε''_{irr} permits now the measurement of a RF conductivity of several S/m, at least three orders of magnitude higher than before irradiation. We wish to mention here that the comparison of the measurements was done on one fixed frequency, $f=10$ GHz, as we observed a certain frequency dependence in the ε determination. In fact, ε' was roughly constant between 7 and 15 GHz, while ε'' was proportional to f. Note that an effective-medium model of the Maxwell-Garnett type,[26] describing the specimen as an assembly of metallic particles embedded in an insulating matrix, predicts precisely such a behavior. The annealing is shown in Fig. 9, indicating that the radiation-induced $\Delta\varepsilon'$, $\Delta\varepsilon''$ recover more or less simultaneously with the disappearance of the colloid line, at $T_{ann}=350$ °C.

E. X-ray observation

We have examined several specimens, irradiated together with those measured by EPR, through x-ray diffractometry. In particular, one sample (called e-17) was irradiated at $T_{irr}=90$ K, another (e-19) at 275 K, and their lattice constants, a, determined after crushing them into powder. A comparison with three nonirradiated Li_2O specimens treated otherwise in the same way (origin, preliminary anneal and storage) showed a slight increase of a for the sample e-17 after irradiation at 90 K, but a decrease for e-19 irradiated near room temperature (cf. Table I). At the same time, the width of selected lines in the x-ray diffraction spectrum increased by about 10% for e-17 and by 40% for e-19, corresponding roughly to the ratio between the bombarding electron fluences, i.e., the induced lattice damage. These preliminary results, especially the apparent contraction after

TABLE I. Lattice parameters and x-ray linewidths.

	a (Å)	$\Delta\Theta(220)$[a]
Non-irr. (average of 3)	4.6126(2)	0.103(2)
e-17 (T_{irr}=90 K)	4.6130	0.113(3)
e-19 (T_{irr}=275 K)	4.6116	0.142(5)

[a]Full width at half maximum of the (220) line at $2\Theta=66.5°$.

introduction of lithium colloids, remain to be confirmed and will be discussed in a later paper treating single-crystal data.

IV. DISCUSSION

A. Creation of F^+ centers

The defects introduced after 1 MeV electron irradiation have the clear cut hyperfine signature of the F^+ centers characterized by Noda *et al.*[15] following an in-pile thermal neutron irradiation at a temperature somewhere between 50 and 100 °C. Their introduction rate was given as initially 4 F^+ cm^{-1} per neutron for a fluence of 4×10^{16} n/cm^2, decreasing rapidly to 0.2 F^+ cm^{-1} per neutron for 1.7×10^{19} n/cm^2. We have determined the number of F^+ centers corresponding to the intensity of the F^+ signal in our EPR spectra, by comparing a calibrated $CuSO_4$ signal, and find, for example, for the 21 K and 90 K irradiations, as the simplest cases exhibiting a pure F^+ signal, a concentration of 1.15×10^{-4} F^+ per Li_2O molecule in the former sample and of 1.5×10^{-4} F^+ per molecule in the latter, corresponding to a damage rate by 1 MeV electrons of 5.8×10^{-2} F^+ cm^{-1} per electron at T_{irr} = 21 K and 0.8×10^{20} e^-/cm^2 and 8.9×10^{-2} F^+ cm^{-1} per electron at T_{irr}=90 K and 0.3×10^{20} e^-/cm^2, possibly indicating a small saturation effect for the former.

Assuming the absence of a notable radiolytical process (as suggested by Noda *et al.*[15] following a negative gamma irradiation) and, thus, a purely collisional displacement mechanism for the creation of F^+ centers, one can estimate their concentration in an electron irradiation using the tables of Oen[27] who had calculated the cross sections for atomic displacement for a great number of elements. The threshold energy for displacing an oxygen atom in Li_2O has not been determined experimentally; we are, therefore, taking a value measured by Pells in MgO,[28] where similar damage mechanisms can be considered to a good approximation, $T_d^0=53$ eV, giving a cross section of 7 barns for 1 MeV electrons. For the two fluences used above, we obtain 5.6×10^{-4} per molecule in the former case and 2.1×10^{-4} per molecule in the latter. The very reasonable order-of-magnitude agreement of these calculated values and the measured concentrations given above are a strong indication for the predominance of a collisional displacement mechanism for the creation of F^+ centers.

B. F^+ aggregates

The central line near $g=2.0030$, which develops during the annealing process and is already present at room temperature in the case of the 150 and 200 K irradiations (Figs. 4 and 6), can be attributed to small aggregates of F^+ centers, the latter probably becoming mobile near 150 K. The parallel increase of its intensity and decrease of the F^+ signal (Figs. 3, 5, and 7), with a maximum just at the vanishing of the latter, together with the color change accompanying its emergence, supports this proposal. The decreasing linewidth for higher annealing temperatures, $T_{ann}\geqslant400$ °C, is possibly caused by growing aggregate size before disappearing (at 600–650 °C) due to arriving mobile Li vacancies.[29]

Finally, we wish to remark that the line at $g=2.003(1)$, superimposed upon the F^+ signal observed by Noda's group in Li_2O irradiated with neutrons[13,16,17] or with oxygen ions[16,19] and attributed by them to metallic lithium colloids, possesses all the characteristics of our central line: a g value between 2.003 and 2.004, a linewidth between 0.2 and 1 mT, and an identical recovery behavior. This is probably also the reason why Masaki *et al.*[17] observe only the $g=2.003$ line after a neutron bombardment at $T_{irr}=650$ K; the F^+ centers formed under irradiation have already vanished at this temperature. The strongest arguments, however, against the assignment of the $g=2.003$ line to metallic colloids is its temperature dependence (never reported by Noda's group), which is Curie-like in our experiments, and the practically unchanged dielectric constant of the samples of Secs. III A to III C, in striking contrast to those containing colloids (Sec. III D).

C. Li colloids

The $g=2.0023$ line showing up after the room-temperature irradiation replaces apparently the F^+ signal, indicating an agglomeration of these simpler defects into metallic clusters. This is a clear-cut manifestation of lithium colloids in Li_2O. The dramatic ε increase is an additional convincing argument for the presence of metallic particles. The number of spins corresponding to the intensity of the colloid line in the sample of Sec. III D was determined, taking into account its Pauli-like temperature (in)dependence and applying a Fermi temperature $T_F=1.2\times10^5$ K to be 1.9×10^{-5} per molecule; this is a reasonable order of magnitude lower than that of the primary F^+ centers estimated above, in view of possible elimination of the latter during their migration.

The colloid line disappears after annealing at 350 °C (see Fig. 9), but in a broader stage than the simultaneously vanishing ε increase, $\Delta\varepsilon'$ and $\Delta\varepsilon''$. One possible reason for this behavior could be an initial colloid coalescence, conserving the dielectric characteristics of the sample, until T_{ann}=200–250 °C, before their final breakup and disappearance. As indicated above, the not quite regular line shape might imply a distribution of colloid sizes, but this remains to be confirmed.

Concluding, we wish to emphasize that, after the observation of metallic lithium colloids in LiF (Refs. 7–9) and LiH,[10–12] the present experiments provide their manifestation in another compound, Li_2O. One can only wonder about the reasons why Noda and his co-workers had not succeeded in observing metallic clusters in their various irradiation experiments. As their T_{irr} was often near room temperature and, thus, the mobility of created F^+ centers sufficient for their

agglomeration, we can only suggest the different impurity contents as a possible argument. Indeed, their samples being much purer[15] than ours, the possibility of trapping mobile point defects such as Li vacancies and interstitials by impurities and, hence, of permitting the F^+ agglomeration into colloids might be larger in our case than in theirs. [Actually, Noda *et al.* had already noted that the $g=2.0030$ line was present in sintered pellets of Li_2O (Ref. 13) but not in single crystals[15] attributing to the grain boundaries a role in the precipitation process.] More generally, unambiguous observations of intrinsic metallic colloids in other oxides were, as far as we know, reported until now only for Al in α-Al_2O_3 in a high-voltage electron microscope,[30] after unsuccessful efforts with MgO (Ref. 28), Li_2ZrO_3 (Ref. 31), and $LiAlO_2$.[31,32]

ACKNOWLEDGMENTS

We wish to thank Ghita Geoffroy for the x-ray-diffraction analysis. This work was supported in part by the European Fusion Technology Program, Task UT-M-CM1.

[1] F. Beuneu and P. Monod, Phys. Rev. B **18**, 2422 (1978); P. Monod and F. Beuneu, *ibid* **19**, 911 (1979).
[2] G. Feher and F. Kip, Phys. Rev. **98**, 337 (1955); F. J. Dyson, *ibid* **98**, 349 (1955).
[3] A. E. Hughes and S. C. Jain, Adv. Phys. **28**, 717 (1979).
[4] M. Lambert and A. Guinier, C. R. Acad. Sci. Paris **246**, 1678 (1958).
[5] P. J. Ring, J. G. O'Keefe, and P. J. Bray, Phys. Rev. Lett. **1**, 453 (1958).
[6] Y. W. Kim, R. Kaplan, and P. J. Bray, Phys. Rev. **117**, 740 (1960).
[7] M. Lambert, Ch.Mazières, and A. Guinier, J. Phys. Chem. Solids **18**, 129 (1961).
[8] A. T. Davidson, J. D. Comins, T. E. Derry, and F. S. Khumalo, Rad. Eff. **98**, 305 (1986).
[9] N. Seifert, S. Vijayalakshmi, Q. Yan, J. L. Allen, A. V. Barnes, R. G. Albridge, and N. H. Tolk, Phys. Rev. B **51**, 16 403 (1995).
[10] W. T. Doyle, D. J. E. Ingram, and M. J. A. Smith, Proc. Phys. Soc. **74**, 540 (1959).
[11] F. E. Pretzel, D. T. Vier, E. G. Szklarz, and W. B. Lewis, Los Alamos Scientific Laboratory Report No. LA-2463 (1961).
[12] A. Berthault, S. Bedere, and J. Matricon, J. Phys. Chem. Solids **38**, 913 (1977).
[13] K. Noda, K. Uchida, T. Tanifuji, and S. Nasu, J. Nucl. Mater. **91**, 234 (1980).
[14] K. Uchida, K. Noda, T. Tanifuji, Sh. Nasu, T. Kirihara, and A. Kikuchi, Phys. Status Solidi A **58**, 557 (1980).
[15] K. Noda, K. Uchida, T. Tanifuji, and S. Nasu, Phys. Rev. B **24**, 3736 (1981).
[16] K. Noda, T. Tanifuji, Y. Ishii, H. Matsui, N. Masaki, S. Nasu, and H. Watanabe, J. Nucl. Mater. **122/123**, 908 (1984).
[17] N. M. Masaki, K. Noda, H. Watanabe, R. G. Clemmer, and G. W. Hollenberg, J. Nucl. Mater. **212/215**, 908 (1994).
[18] K. Noda, Y. Ishii, H. Matsui, and H. Watanabe, J. Nucl. Mater. **133/134**, 205 (1985).
[19] K. Noda, Y. Ishii, H. Matsui, and H. Watanabe, Rad. Eff. **97**, 297 (1986).
[20] K. Noda, Y. Ishii, H. Matsui, H. Ohno, S. Hirano, and H. Watanabe, J. Nucl. Mater. **155/157**, 568 (1988).
[21] K. Noda, Y. Ishii, H. Matsui, H. Ohno, and H. Watanabe, J. Nucl. Mater. **179/181**, 835 (1991).
[22] Y. Asaoka, H. Moriyama, K. Iwasaki, K. Moritani, and Y. Ito, J. Nucl. Mater. **183**, 174 (1991).
[23] J. M. Baker, A. Cox, A. J. O'Connell, and R. C. C. Ward, J. Phys. Condens. Matter **3**, 6189 (1991).
[24] P. Vajda and F. Beuneu, Nucl. Instrum. Methods (to be published).
[25] L. Pagès, E. Bertel, H. Joffre, and L. Sklavenitis, Commissariat à l'Energie Atomique Report No. CEA-R-3942 (1970).
[26] R. Landauer, in *Electrical Transport and Optical Properties of Inhomogeneous Media*, edited by J. C. Garland and D. B. Tanner, AIP Conf. Proc. No. 40 (AIP, New York, 1978), p. 2.
[27] O. S. Oen, Oak Ridge National Laboratory Report No. ORNL-4897 (1973).
[28] G. P. Pells, Rad. Eff. **64**, 71 (1982).
[29] Z. H. Xie, M. E. Smith, J. H. Strange, and C. Jaeger, J. Phys.Condens. Matter **7**, 2479 (1995).
[30] T. Shikama and G. P. Pells, Philos. Mag. A **47**, 369 (1983).
[31] M. H. Auvray-Gély, A. Dunlop, and L. W. Hobbs, J. Nucl. Mater. **133/134**, 230 (1985).
[32] M. H. Auvray-Gély, A. Perez, and A. Dunlop, Philos. Mag. B **57**, 137 (1988).